Calculation of Aerosol Collection in Fluidized Filter Beds

A method is proposed for calculating aerosol collection in fluidized filter beds. The method employs the bubble assembly model of fluidization and considers the bed to be a series of compartments, each of which comprises two or three phases. Aerosol collection is assumed to occur in these phases in accordance with existing theories of particle deposition. The validity of the method is tested against available experimental data.

K. USHIKI and CHI TIEN

Department of Chemical Engineering and Materials Science
Syracuse University
Syracuse, NY 13210

SCOPE

The study is concerned with the development of a method which can be applied for the prediction of the performance of fluidized-bed filters in removing fine particles from gaseous streams. Unlike fixed-bed filters, fluidized filters have the advantage of operating as a continuous process with much greater gas throughout. At the same time, fluidized filtration represents a more complex physical phenomena and consequently its description is more difficult than that of fixed-bed filtration.

The method developed in this work is based on the bubble assemblage concept of Kato and Wen (1969). The bed is considered to be a series of compartments, which each comprises either two or three phases, depending on the fluidization state. Aerosol collection takes place in the dense phase (or phases) with neither axial dispersion nor complete mixing. There are interchanges of gases as well as a net flow of gases from one phase to another. The latter condition makes it possible to consider gas flow reversal, which has been noted by previous investigators.

A detailed discussion of the differences between the present method and an earlier one (Peters et al., 1982a) is presented as part of the study. In addition, extensive comparisons between predictions based on the present method and available data are made to demonstrate the validity and accuracy of the method.

CONCLUSIONS AND SIGNIFICANCE

The method developed in this work makes it possible to predict the performance of fluidized filter beds and to relate this performance in terms of existing theories of fluidization and particle collection. The validity of the method, specifically the application of the bubble assembly model in describing gas-solids fluidization and the use of the recently developed collection efficiency expression (Pendse and Tien, 1982) is substantiated through the good agreement between the calculations and available experimental data.

INTRODUCTION

The application of granular filter beds for removing fine particles from gaseous streams is a common engineering practice. A survey conducted by the National Argonne Laboratory (Juvinall et al., 1970) indicates that the use of granular filters covers practically all the important segments of process and chemical industries, especially mineral and nuclear fuel processing. More recently, granular filtration has also attracted significant interest as a candidate process for high-temperature and high-pressure gas cleaning.

The advantage of granular filtration resides mainly in its relatively high collection efficiency and in the availability of granular substances which are immune to adverse environments. The disadvantage of conventional granular filtration in the fixed-bed mode is that the process operates inherently in an unsteady state. During filtration, a fixed-bed granular filter experiences significant changes in its collection efficiency and in the pressure drop across the bed. As the bed becomes clogged, it requires frequent regeneration.

A possible alternative, which could overcome these advantages, is to operate the filter in either moving-bed or fluidized-bed modes. The continuous withdrawal of filter grains that may take place with these two modes makes it possible to maintain filtration as a steady-state process.

A number of investigations on aerosol collection in fluidized filters have been conducted during the past three decades (Meissner and Mickley, 1949; Scott and Guthrie, 1959; Philney and Erikson, 1968a,b; Knettig and Beechmans, 1974; McCarthy et al., 1976; Patterson and Jackson, 1977; Doganoglu et al., 1978). In the more recent years the applications of external force to enhance filtration has also been explored (Ciborows and Zakowski, 1977; Ciborovsky and Wlodarsky, 1962; Zahedi and Melcher, 1976, 1977). Although these studies covered a wide spectrum of interest, the interpretation of these results and their eventual application as a basis for rational design must be handled with care because of the uncertainties associated with experimental work of this kind (Doganoglu et al., 1978).

Another major difficulty in interpreting data is the lack of a proper theoretical framework which describes fluidized filtration in a simple, yet realistic manner. Some of the previous investigations have proposed models. In most cases, however, these models are nothing more than empirical correlations based on limited data. Only recently have efforts been made to relate fluidized filtration to the fundamental theories of fluidization and particle collection.

K. Ushiki is on leave from the Department of Chemical Engineering, Kyoto University, Kyoto, Japan.

Doganoglu et al. (1978) applied the two-phase theory of fluidization for the interpretation of their filtration data with the use of two empirical parameters. However, there was no attempt to develop any theories or correlations for estimating these parameters.

A conceptually complete model of aerosol filtration in fluidized filters was formulated by Peters, Fan and Sweeney (1982a). The bubble assembly model of fluidization (Kato and Wen, 1969) was used to characterize the fluid mechanical behavior of the bed. The bed is assumed to be composed of a series of compartments which, in turn, comprises three phases: bubble, cloud and emulsion. Aerosol collection takes place in both the cloud and emulsion phases with the supposition that aerosol concentrations in both phases are uniform. The extent of aerosol collection was estimated using collection efficiencies based on the isolated sphere model.

The significance of the work of Peters et al. (1982a) is in their attempts to describe fluidized filter performance using the basic principles of fluidization and particle collection. Therefore, their work offers a rational and conceptually sound framework. Some of the assumptions used in their analysis, however, require further clarification. The gas velocities through and the volume fractions of each phase were assumed to be constant throughout the bed. Trial calculations using their model indicate that, under certain conditions, the volume fraction of the emulsion phase may become negative, which is clearly a physical impossibility. Moreover, in light of some recent data (Albert, 1982), the assumption of uniform gas concentration in the emulsion phase appears questionable. Also, the collection efficiency based on the isolated sphere model that was used in the work of Peters et al. gives results substantially at variance with experimental data (Tien, 1982).

This paper represents a natural extension of the work of Peters et al. (1982a). The basic concept of bubble assemblage is explored. There are substantial differences, however, between the present work and the earlier analysis of Peters et al., both in the bed description and in the consideration of aerosol collection. For the description of the structures of fluidized filters in this work, the volume fractions and gas velocities of each phase are not considered constant but vary with bed height. Hence, there exists not only gas interchange between phases but also the possibility of net gas flow between phases. Furthermore, the number of phases present in each compartment is determined by the condition of the state of fluidization. The previously mentioned problem of having a negative value for the volume fraction of the emulsion phase is, therefore, avoided. For aerosol collection, the structure of both emulsion and cloud phases is described by the constricted-tube model (Payatakes et al., 1973; Tien and Payatakes, 1979; Tien, 1982). The collection efficiency expression of Pendse and Tien (1982) is then used to estimate the extent of aerosol collection.

STRUCTURE OF MODELS

The bubble assembly modes of Kato and Wen (1969) as modified by Peters, Fan and Sweeny (1982a,b) are adopted with several modifications as follows:

(1) The number of phases present in each compartment is not assumed *a priori* but is determined by calculating the volume fraction of the cloud phase using the model of Murray (1965).

(2) In contrast to the work of Peters et al. (1982a) which used average values, here the structures and the velocities of each phase in a compartment are allowed to vary.

(3) The flow pattern within the cloud phase is assumed to be well mixed. The emulsion phase is considered to be similar to that of packed bed with no axial dispersion.

(4) The height of each compartment is assumed to be the same as the bubble size if the compartment comprises two phases (bubble and dense phase). It is taken to be the height of the cloud diameter if the compartment comprises three phases (bubble, cloud and emulsion).

A schematic diagram depicting the assumed fluidized-bed structure is shown in Figure 1. The quantitative specification of the bed structure is described as follows.

Two-Phase Regime

The two-phase regime applies to the lower part of a bed, where formation of gas bubbles originates. The two phases present are the bubble phase (Phase 1) and the dense phase (Phase 2). For description, the compartment heights, the gas velocities and the volume fractions of each phase, and the net gas flow rate between the two phases need specification.

The compartment height in the two-phase region is taken to be the gas bubble diameter, D_1, which can be estimated from the Mori-Wen correlations (1975).

$$\frac{D_{1_m} - D_1}{D_{1_m} - D_{1_0}} = \exp(-0.3h/D_R) \tag{1}$$

where

$$D_{1_m} = 0.652[S(u_o - u_{mf})]^{2/5} \tag{2}$$

$$D_{1_0} = 0.347\left[\frac{S(u_0 - u_{mf})}{N_D}\right]^{2/5} \tag{3a}$$

for perforated distributor plates,

$$D_{1_0} = 0.00376(u_0 - u_{mf})^2 \tag{3b}$$

for porous distributor plates. The correlation is valid over the following variable ranges: $0.5 < u_{mf} < 20$ cm/s; $60 < D_c < 450$ μm; $u_0 - u_{mf} < 48$ cm; $D_R < 130$ cm; u_0 and u_{mf} are the superficial velocity and the minimum fluidization velocity, respectively. S is the cross-sectional area of the bed, and D_R, the diameter of the bed. The bubble size (diameter) according to Eq. 1 increases along the axial distance measured from the distribution plate, h. The bed height corresponding to the position of the nth compartment (from the distributor plate to the midpoint of the compartment) h_n, is given as

$$h_n = \sum_{i=1}^{n-1} D_{1_i} + D_{1_n}/2 \tag{4a}$$

where D_{1_i} is the bubble diameter of the ith compartment. The linear gas velocity of the bubble phase (i.e., Phase 1) of the nth compartment, u_{1_n} may be written as

$$U_{1_n} = u_{1_{sn}} + 0.711\sqrt{gD_{1_n}} \tag{5}$$

The derivation of the above equation is given in Appendix A. By definition, $u_{1_{sn}}$ is related to u_{1_n} by the expression

$$u_{1_{sn}} = u_{1_n}\delta_{1_n}\epsilon_{1_n} \tag{6}$$

where δ_{1_n} and ϵ_{1_n} are the volume fraction of Phase 1 (bubble phase) and the porosity of Phase 1 of the nth compartment, respectively. If ϵ_{1_n} is taken to be unity, one has

$$u_{1_{sn}} = u_{1_n}\delta_{1_n} \tag{7}$$

The volume fraction of the bubble Phase 1 in the nth compartment, δ_{1_n}, can be found from the following reasoning. The volume of the nth compartment is SD_{1_n}. The volume of solids present in the compartment is $SD_{1_n}(1 - \epsilon_n)$, where ϵ_n is the porosity of the bed at the location of the nth compartment. If one assumes that the porosity of the dense phase is ϵ_{mf}, namely the porosity at the incipience of fluidization, the bubble-phase volume is found to be

$$SD_{1_n} - SD_{1_n}(1 - \epsilon_n)/(1 - \epsilon_{mf}) = SD_{1_n}\left(\frac{\epsilon_n - \epsilon_{mf}}{1 - \epsilon_{mf}}\right)$$

and the volume fraction of the bubble phase in the nth compartment, δ_{1_n}, becomes

$$\delta_{1_n} = \frac{\epsilon_n - \epsilon_{mf}}{1 - \epsilon_{mf}} \tag{8}$$

The volume fraction of the dense phase in the compartment, δ_{2_n}, becomes

$$\delta_{2_n} = 1 - \delta_{1_n} \text{ if } \left(\frac{\epsilon_n - \epsilon_{mf}}{1 - \epsilon_{mf}}\right)\left(\frac{u_{mf}}{\epsilon_{mf}u_{1_n} - u_{mf}}\right) > 1 - \delta_{1_n} \tag{9}$$

The quantity $(\epsilon_n - \epsilon_{mf}/1 - \epsilon_{mf})(u_{mf}/\epsilon_{mf}u_1 - u_{mf})$, as shown

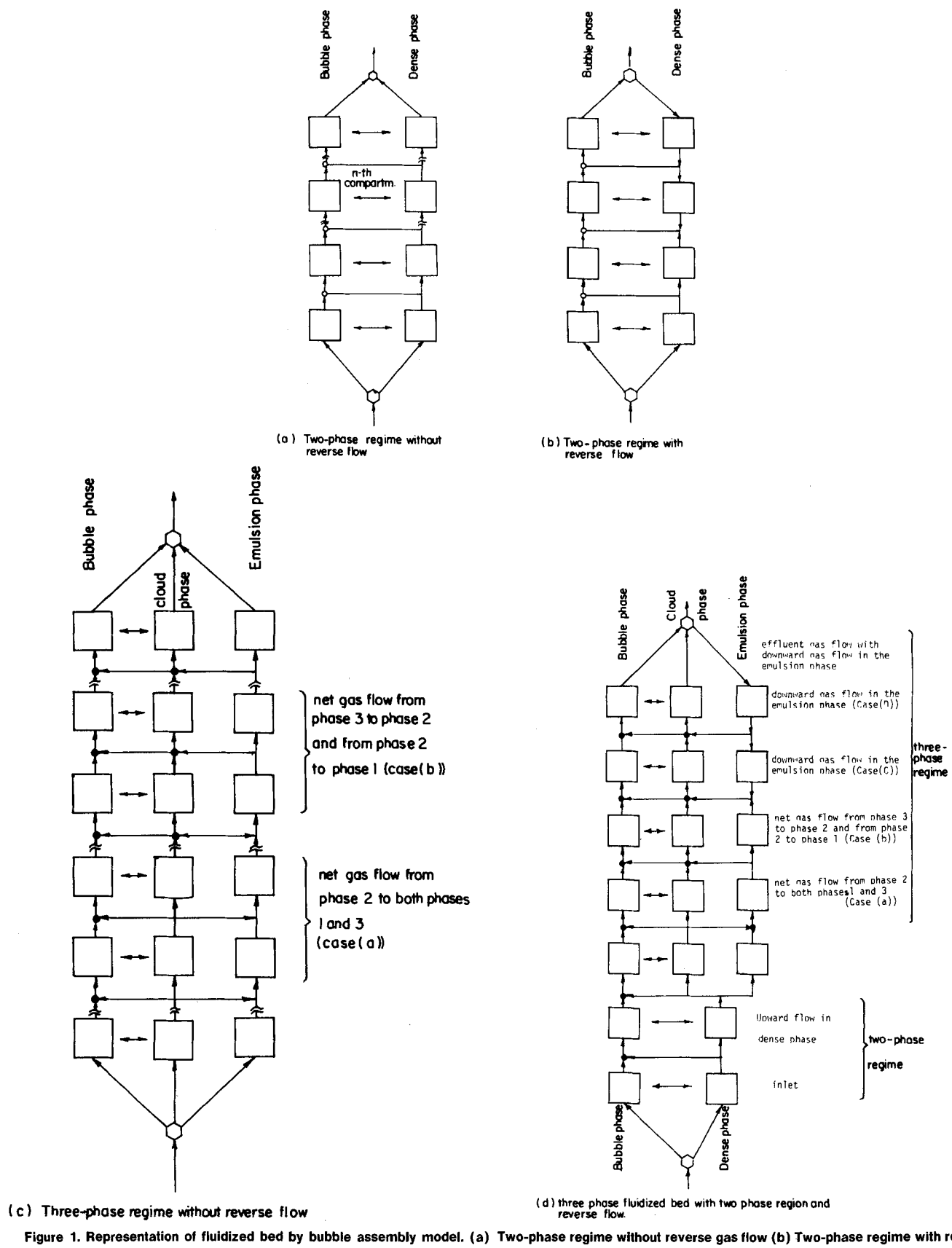

Figure 1. Representation of fluidized bed by bubble assembly model. (a) Two-phase regime without reverse gas flow (b) Two-phase regime with reverse gas flow (c) Three-phase regime without reverse gas flow (d) Both two-phase and three-phase regimes with reverse gas flow

later, is the volume fraction of the cloud phase according to the three-phase model. The inequality condition, therefore, is the criterion which determines the transition from the two-phase regime to the three-phase regime. The necessity of this provision is obvious; without it, one may have the situation in which $\delta_{1_n} + \delta_{2_n} > 1.0$, or $\delta_{3_n} \leq 0$, which, of course, is a physical impossibility. This very difficulty may occur if the bed is described by the three-phase model throughout its entire length.

Combining Eqs. 5, 7 and 8 and after rearrangement, one has

$$u_{1_n} = \left(\frac{1-\epsilon_{mf}}{1-\epsilon_n}\right)(0.711)\sqrt{gD_{1_n}} \tag{10}$$

and the corresponding superficial velocity, $u_{1_{sn}}$, becomes

$$u_{1_{sn}} = \left(\frac{\epsilon_n-\epsilon_{mf}}{1-\epsilon_n}\right)(0.711)\sqrt{gD_{1_n}} \tag{11}$$

From the continuity requirement, $u_{2_{sn}}$ is found to be

$$u_{2_{sn}} = u_0 - i_{1_{sn}} \tag{12}$$

Both the velocities and the volume fractions are expressed in terms of ϵ_n, which can be estimated from the following relationships (Peters et al., 1980):

$$\epsilon_n = 1 - \frac{L_{mf}}{L}(1-\epsilon_{mf}) \qquad \text{if } h_n \le L_{mf} \tag{13a}$$

$$\epsilon_n = 1 - \frac{L_{mf}}{L}(1-\epsilon_{mf})\left[\exp\frac{-(h_n-L_{mf})}{(L-L_{mf})}\right] \qquad \text{if } h_n \ge L_{mf} \tag{13b}$$

The total bed height, L, is given as

$$L = L_{mf} + \frac{0.76L(u_0-u_{mf})}{u_0 - u_{mf} + 0.71\sqrt{g\overline{D}_1}} \tag{14}$$

where

$$\overline{D}_1 = D_{1_m} - (D_{1_m} - D_{1_0})\exp[-0.15L_{mf}/D_R] \tag{15}$$

The correlations used for estimating u_{mf} and ϵ_{mf} are given in Appendix B. A step-by-step calculation can then be made to determine the compartment dimension and its corresponding position (i.e., h_n) from Eqs. 1 and 4a. The volume fractions and the gas velocities of either phase can be calculated from Eqs. 8, 9, 11 and 12, with ϵ_n estimated from Eqs. 13a and 13b. This calculation proceeds until the total bed length, L, is covered or until the inequality criterion of Eq. 9 is no longer obeyed. In the latter case, this condition means that the two-phase model can no longer be used beyond this point.

For the two-phase model, there is a continuous exchange of gas between the two phases. For convenience, one may divide this gas exchange into two parts: (a) a net flow of gas from one phase to another prior to the gas's entry into a compartment; and (b) an interchange of gas (but no net flow) between the two phases within each compartment. The first type of exchange is necessary since the value of $u_{1_{sn}}$ is not assumed to be constant but changes with bed height, Figure 2.

The interchange between phases can be estimated using the gas interchange coefficient concept. Based on the work of Murray (1965) modified by Sit and Grace (1981), the gas interchange coefficient between the two phases can be expressed as (Peters et al., 1982b).

$$F_{12n} = 2\left(\frac{u_{mf}}{D_{1_n}}\right) \tag{16}$$

and the volume of gas interchanged between the two phases per unit time, F_{v_n}, is given as

$$F_{vn} = F_{12_n}V_{1_n} = 2\left(\frac{u_{mf}}{D_{1_n}}\right)(D_{1_n})\cdot(S)\delta_{1_n} = 2u_{mf}S\frac{\epsilon_n-\epsilon_{mf}}{1-\epsilon_{mf}} \tag{17}$$

and the corresponding bed height, h, becomes

$$h_n = \sum_{i=1}^{k} D_{1_n} + \sum_{j=k+1}^{n-1} D_{2_j} + D_{2_n}/2 \tag{4b}$$

assuming that the two-phase model applies up to the kth compartment.

Three-Phase Regime

The failure to obey the inequality criterion of Eq. 9 signals the emergence of two distinct dense phases. The use of the three-phase model is then required. The compartment is assumed to comprise three phases: bubble phase (Phase 1), cloud phase (Phase 2), and emulsion phase (Phase 3).

The compartment height for the three-phase regime is defined to be the same as the cloud diameter, D_{2_n}, which is given as

$$D_{2_n} = D_{1_n}\left(\frac{\delta_{2_n}+\delta_{1_n}}{\delta_{1_n}}\right)^{1/3} \tag{18}$$

with D_{1_n} given by Eq. 1. The volume fraction of the bubble phase, δ_{i_n}, is given by Eq. 8 as before. The volume fraction of the cloud and emulsion phases become, respectively,

$$\delta_{2_n} = \left(\frac{\epsilon_n-\epsilon_{mf}}{1-\epsilon_{mf}}\right)\left(\frac{u_{mf}}{\epsilon_{mf}u_{1_n}-u_{mf}}\right) \tag{19}$$

and

$$\delta_{3_n} = 1 - \delta_{1_n} - \delta_{2_n} \tag{20}$$

As above, the total compartment porosity, ϵ_n, is given by Eq. 13a or 13b. The porosities of the three phases are assumed to be

$$\epsilon_{1_n} = 1 \qquad \epsilon_{2_n} = \epsilon_{3_n} = \epsilon_{mf} \tag{21}$$

From the knowledge that

$$u_{1_n} = \frac{1-\epsilon_{mf}}{1-\epsilon_n}(0.711)\sqrt{gD_{1_n}} \tag{10}$$

The gas velocities of each phase are known to be

$$u_{1_{sn}} = u_{1_n}\delta_{1_n}\epsilon_1 = 0.711\sqrt{gD_{1_n}}\left(\frac{\epsilon_n-\epsilon_{mf}}{1-\epsilon_n}\right) \tag{11}$$

$$u_{2_{sn}} = u_{1_{sn}}\left(\frac{\delta_{2_n}\epsilon_{2_n}}{\delta_{1_n}\epsilon_{1_n}}\right) = u_{1_{sn}}\left(\frac{\delta_{2_n}}{\delta_{1_n}}\right)\epsilon_{2_n} \tag{22}$$

$$u_{3_{sn}} = u_0 - u_{1_{sn}} - u_{2_{sn}} \tag{23}$$

The net gas flow from the cloud phase to the bubble and emulsion phases are, from cloud to bubble phase, $S(u_{1_{sn}} - u_{1_{sn-1}})$ and, from cloud to emulsion phase, $S(u_{3_{sn}} - u_{3_{sn-1}})$

The gas interchange coefficient between the cloud and bubble phases, F_{12}, is the same as that given by Eq. 16. According to Kunii and Levenspiel (1968), the gas interchange between the cloud and emulsion phase is negligible. The rate of the gas interchange between the cloud and bubble phases is

$$F_{v_n} = (F_{12})V_{1_n} = 2\left(\frac{u_{mf}}{D_{1_n}}\right)(\delta_{1_n})SD_{2_n}$$
$$= 2Su_{mf}\left[\frac{\epsilon_n-\epsilon_{mf}}{1-\epsilon_{mf}}\right]\left[\frac{\epsilon_{mf}u_{1_n}}{\epsilon_{mf}u_{1_n}-u_{mf}}\right]^{1/3} \tag{24}$$

EQUATIONS OF AEROSOL COLLECTION

Equations describing the extent of particle collection can be obtained by making mass balances of aerosol particles for each phase.

Two-Phase Regime

The gas velocities in both phases are uniform, Figures 2a–c. The figures correspond to the three possible situations for a given compartment (except for the first and last).

Case(a): Upward Flow in Dense Phase. The aerosol mass balance equations for each phase can be written as follows:

Bubble Phase

$$Su_{1_{sn-1}}c_{1_{n-1}} + S(u_{1_{sn}} - u_{1_{sn-1}})c_{2_{n-1}} + F_{v_n}c_{2_n} + Su_{1_{sn}}c_{1_n} + F_{v_n}c_{1_n} \tag{25}$$

Dense Phase

$$Su_{2_{sn}}c_{2_{n-1}} + F_{v_n}c_{1_n} = Su_{2_{sn}}c_{2_n} + F_{v_n}c_{2_n} + M_{2_n} \tag{26}$$

where M_{2_n} is the rate of particle collection.

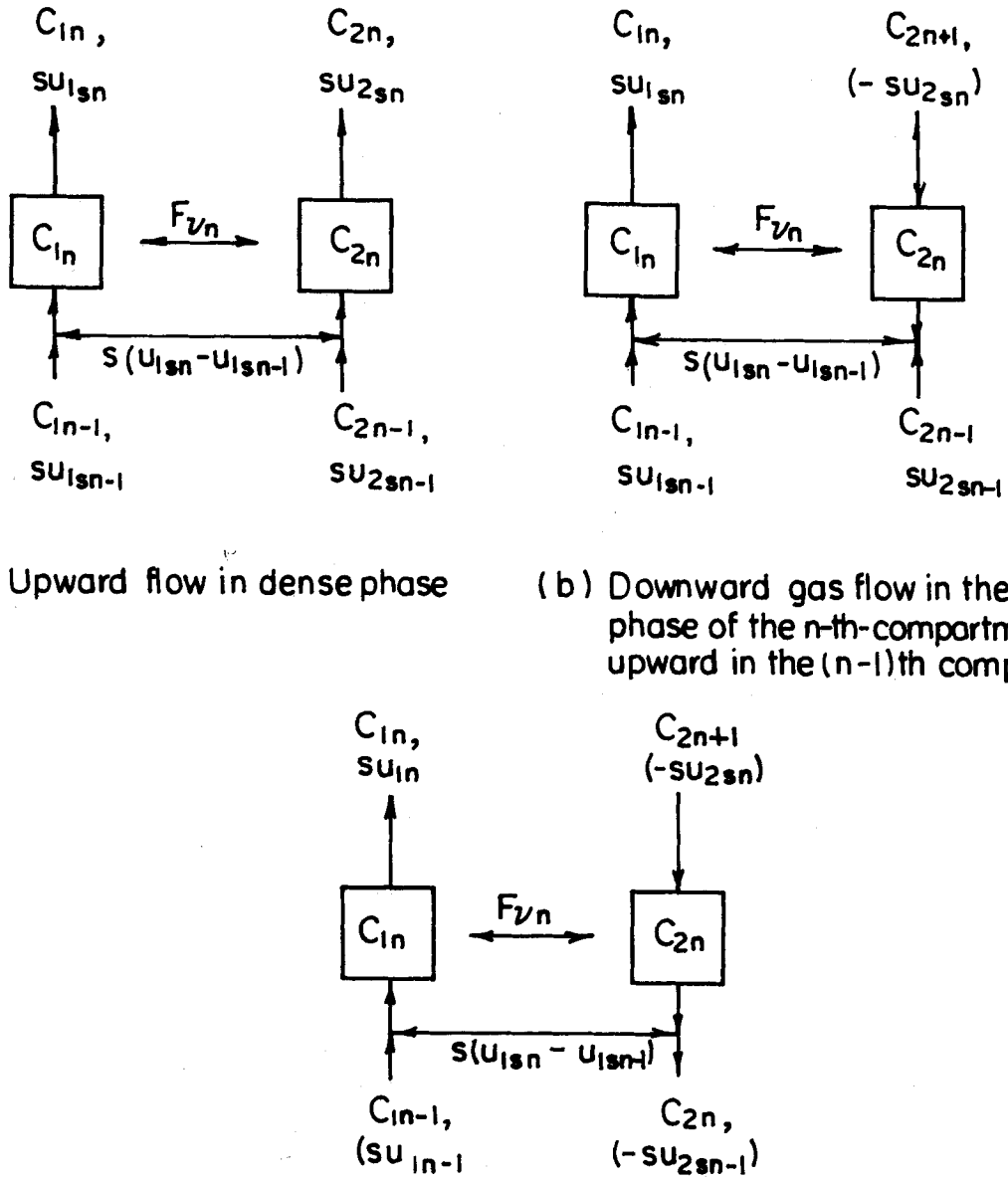

Figure 2. Three possible flow structures in two-phase regime.

To estimate M_{2_n}, the dense phase is considered structurally as a packed bed and is described by the constricted tube model (Payatakes et al., 1973). The volumetric flow rate per unit cell (i.e., per tube), q, is given as

$$q = \left(\frac{u_{2_{sn}}}{\delta_{2_n}}\right) \Big/ N_c \tag{27}$$

where N_c is the number of constricted tubes per unit cross section of bed. The axial distance of the bed corresponding to a unit cell is l (Payatakes et al., 1973). l is given as

$$l = \left[\frac{\pi}{6}\frac{1}{1-\epsilon}\right]^{1/3} d_c \tag{28}$$

Thus, the volume occupied by a unit cell in the dense phase is l/N_c, with $\epsilon = \epsilon_{mf}$ in Eq. 28. If the number of aerosol particles collected in a unit cell is m_c, the volume of deposited particles per unit volume of dense phase, σ, or the specific deposit, becomes

$$\sigma = \frac{(m_c)\left(\frac{\pi}{6}d_p^3\right)}{(l/N_c)} \tag{29}$$

when d_p is the diameter of the aerosol particle.

The rate of particle collection, $\partial\sigma/\partial\theta$, is given as

$$\frac{\partial\sigma}{\partial\theta} = \left(\frac{\pi}{6}d_p^3\right)\frac{N_c}{l}\frac{dm_c}{dm_{\text{in}}}\frac{dm_{\text{in}}}{d\theta} \tag{30}$$

where m_{in} is the number of particles entering into the unit cells and is given as

$$m_{\text{in}} = \int_0^\theta \left[(q)\cdot C \Big/ \left(\frac{\pi}{6}d_p^3\right)\right]\cdot d\theta \tag{31}$$

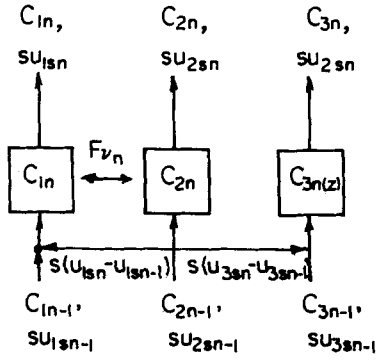

(a) Net gas flow from phase 2 to both phase 1 and 3

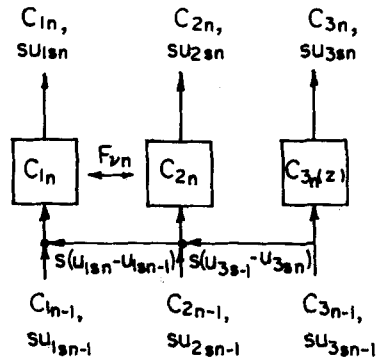

(b) Net gas flow from phase 3 to phase 2 and from phase 2 to phase 1

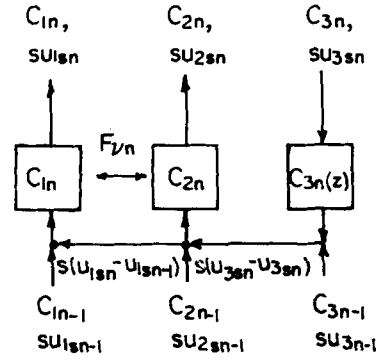

(c) Downward gas flow in the emulsion phase of the n-th compartment

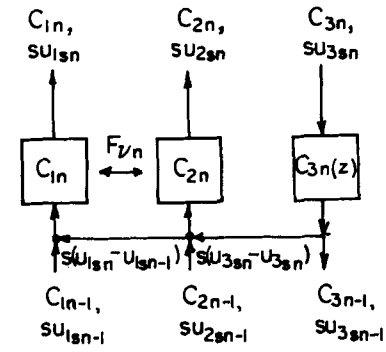

(d) Downward gas flow in the emulsion phase of both n-th and (n-1) th components

Figure 3. Four possible flow structures in three-phase regime.

By definition, dm_c/dm_{in} is the collection efficiency of the unit cell, or

$$\eta = \frac{dm_c}{dm_{in}} \tag{32}$$

Combining Eqs. 27, 30, 31, and 32, one has, for the dense phase of the nth compartment,

$$\left(\frac{\partial \sigma}{\partial \theta}\right)_n = \frac{u_{2_{sn}}}{\delta_{2_n}} c_{2_n} \frac{1}{l} \eta \tag{33}$$

The volume of the dense phase in the nth compartment is $SD_{1n}\delta_{2_n}$. Accordingly, M_{2_n} becomes

$$M_{2_n} = (SD_{1_n}\delta_{2_n})\left(\frac{\partial \sigma}{\partial \theta}\right)_n = (u_{2_{sn}})c_{2_n}\left(\frac{1}{l}\right)\eta SD_{1_n} \tag{34}$$

The collection efficiency of the unit cells, η, can be found from the equation proposed by Pendse and Tien (1982) (Appendix C).

Case (b): Downward Gas Flow in Dense Phase of the nth Compartment Upward in $(n-1)$th Compartment. The aerosol mass balance equations can be written as follows. The physical situation is depicted in Figure 2b.

Bubble Phase:

$$Su_{1_{sn-1}}c_{1n-1} + Su_{2_{sn-1}}c_{2n-1} + S(-u_{2_{sn}})c_{2_n} + F_{v_n}c_{2_n} = Su_{1_{sn}}c_{1_n} + F_{v_n}c_{1_n} \tag{35}$$

Dense Phase:

$$S(-u_{2_{sn+1}})c_{2_{n+1}} + F_{v_n}c_{1_n} = S(-u_{2_{sn}})c_{2_n} + F_{v_n}c_{2_n} + (-u_{2_{sn}})c_{2_n}\frac{1}{l}\eta SD_{1_n} \tag{36}$$

Case (c): Downward Gas Flow in Dense Phase of Both nth and $(n-1)$th Compartments. According to Figure 2c, the aerosol mass balance equations are:

Bubble Phase:

$$Su_{1_{sn-1}}c_{1n-1} + S(u_{1_{sn}} - u_{1_{sn-1}})c_{2_n} + F_{v_n}c_{2_n} = Su_{1_{sn}}c_{1_n} + F_{v_n}c_{1_n} \tag{37}$$

Dense Phase:

$$S(-u_{2_{sn}})c_{2_{n+1}} + F_{v_n}c_{1_n} = S(-u_{2_{sn}})c_{2_n} + F_{v_n}c_{2_n} + (-u_{2_{sn}})c_{2_n}\frac{1}{l}\eta SD_{1_n} \tag{38}$$

Three-Phase Regime

As before, the aerosol concentrations in both the bubble and cloud phases are assumed uniform. The emulsion phase is considered to behave as a packed bed with negligible axial dispersion.

Case (a): Net Gas Flow from Cloud Phase to Both Bubble and Emulsion Phases. This situation occurs during the initial stage of the three-phase regime, Figure 3a. The aerosol mass balance

equations for the bubble and cloud phases are:

Bubble Phase:

$$Su_{1_{s_{n-1}}}c_{1_{n-1}} + S(u_{1_{s_n}} - u_{1_{s_{n-1}}})c_{2_{n-1}} + F_{v_n}c_{2_n} = Su_{1_{s_n}}c_{1_n} + c_{1_n}F_{v_n} \quad (39)$$

Cloud Phase:

$$Su_{2_{s_n}}c_{2_{n-1}} + F_{v_n}c_{1_n} = Su_{2_{s_n}}c_{2_n} + F_{v_n}c_{2_n} + u_{2_{s_n}}SD_{2_n}\frac{1}{l}\eta c_{2_n} \quad (40)$$

The last term of the above expression represents the rate of aerosol collection given by Eq. 34, but with D_{2_n} replacing D_{1_n}. To obtain an expression of c_{3_n}, note that the inlet concentration to the emulsion phase results from the combination of two gas streams (Figure 2c) which is equal to

Emulsion-phase particle concentration at the inlet

$$= \frac{u_{3_{s_{n-1}}}c_{3_{n-1}} + (u_{3_{s_n}} - u_{3_{s_{n-1}}})c_{2_{n-1}}}{u_{3_{s_n}}} \quad (41)$$

and, by applying the logarithmic concentration distribution relationship (Tien and Payatakes, 1979), one has

$$c_{3_n} = \frac{u_{3_{s_{n-1}}}c_{3_{n-1}} + (u_{3_{s_n}} - u_{3_{s_{n-1}}})c_{2_{n-1}}}{u_{3_{s_n}}} e^{-\lambda D_{2_n}} \quad (42)$$

where λ is the filter coefficient and is related to the collection efficiency, η, by the relationship (Tien and Payatakes, 1974)

$$\lambda = \frac{1}{l} ln \frac{1}{1-\eta} \quad (43)$$

Case (b): Net Gas Flow from Cloud Phase to Bubble Phase and from Emulsion Phase to Cloud Phase. This case is shown in Figure 3b. For the emulsion phase, the outlet concentration, c_{3_n}, is

$$c_{3_n} = c_{3_{n-1}}e^{-\lambda D_{2_n}} \quad (44)$$

The aerosol mass balance equations for the bubble and cloud phases are

$$Su_{1_{s_{n-1}}}c_{1_{n-1}} + S(u_{1_{s_n}} - u_{1_{s_{n-1}}})\left(\frac{c_{3_{n-1}}(u_{3_{n-1}} - u_{3_n}) + c_{2_{n-1}}u_{2_{s_{n-1}}}}{u_{2_{s_{n-1}}} + u_{3_{s_{n-1}}} - u_{3_{s_n}}}\right) + F_{v_n}c_{2_n} = Su_{1_{s_n}}c_{1_n} + F_{v_n}c_{1_n} \quad (45)$$

Cloud Phase:

$$Su_{2_{s_n}}\left(\frac{c_{3_{n-1}}(u_{3_{s_{n-1}}} - u_{3_{s_n}}) + c_{2_{n-1}}u_{2_{s_{n-1}}}}{u_{2_{s_{n-1}}} + u_{3_{s_{n-1}}} - u_{3_{s_n}}}\right) + F_{v_n}c_{1_n} = Su_{2_{s_n}}c_{2_n} + F_{v_n}c_{2_n} + u_{2_{s_n}}SD_{2_n}\frac{1}{l}\eta c_{2_n} \quad (46)$$

Case (c): Downward Gas Flow in Emulsion Phase of nth Compartment. The physical situation is shown in Figure 3c. To obtain the aerosol mass balance equations, one must first note that the outlet aerosol concentration in the gas stream from the emulsion phase, $(c_{2_{out}})_n$, is

$$c_{3_{out\ n}} = c_{3_n}e^{-\lambda D_{2_n}} \quad (47)$$

The aerosol mass balance equations of the bubble and cloud phases are

Bubble Phase:

$$Su_{1_{s_{n-1}}}c_{1_{n-1}} + S(u_{1_{s_n}} - u_{1_{s_{n-1}}})\left(\frac{u_{2_{s_{n-1}}}c_{2_{n-1}} + u_{3_{s_{n-1}}}c_{3_{n-1}} + (-u_{3_{s_n}})c_{3_n}e^{-\lambda D_{2_n}}}{u_{2_{s_{n-1}}} + u_{3_{s_{n-1}}} + (-u_{3_{s_n}})}\right) + F_{v_n}c_{2_n} = Su_{1_{s_n}}c_{1_n} + F_{v_n}c_{1_n} \quad (48)$$

Cloud Phase:

$$Su_{2_{s_n}}\left[\frac{u_{2_{s_{n-1}}}c_{2_{n-1}} + u_{3_{s_{n-1}}}c_{3_{n-1}} + (-u_{3_{s_n}})c_{3_n}e}{u_{2_{s_{n-1}}} + u_{3_{s_{n-1}}} + (-u_{3_{s_n}})}\right] + F_{v_n}c_{1_n} = Su_{2_{s_n}}c_{2_n} + F_{v_n}c_{2_n} + u_{s_{2_n}}c_{2_n}\frac{1}{l}\eta SD_{2_n} \quad (49)$$

Case (d): Downward gas flow in the emulsion phases of both nth and (n − 1)th compartments. The physical situation is shown in Figure 3d. The aerosol mass balance equations are

Bubble Phase:

$$Su_{1_{s_{n-1}}}c_{1_{n-1}} + S(u_{1_{s_n}} - u_{1_{s_{n-1}}})\left(\frac{u_{2_{s_{n-1}}}c_{2_{n-1}} + (-u_{3_{s_n}} + u_{3_{s_n}} + u_{3_{s_{n-1}}})c_{3_n}e^{-\lambda D_{2_n}}}{u_{2_{s_{n-1}}} + (-u_{3_{s_n}} + u_{3_{s_{n-1}}})}\right) + F_{v_n}c_{2_n} = Su_{1_{s_n}}c_{1_n} + F_{v_n}c_{1_n} \quad (50)$$

Cloud Phase:

$$Su_{2_{s_n}}\frac{u_{2_{s_{n-1}}}c_{2_{n-1}} + (-u_{3_{s_n}} + u_{3_{s_{n-1}}})c_{3_n}e^{-\lambda D_{2_n}}}{u_{2_{s_{n-1}}} + (-u_{3_{s_n}} + u_{3_{s_{n-1}}})} + F_{v_n}c_{1_n} = Su_{2_{s_n}}c_{2_n} + F_{v_n}c_{2_n} + u_{2_{s_n}}c_{2_n}\frac{1}{l}\eta SD_{2_n} \quad (51)$$

Emulsion Phase:

$$c_{3_{n-1}} = c_{3_n}e^{-\lambda D_{2_n}} \quad (52)$$

Effluent Concentration

The effluent concentration, c_{eff}, results from the combination of the gas streams of the individual phases of the last compartment (i.e., Nth). For the various cases considered above, c_{eff} is given as

(a) Two-phase case with upward flow in both phases

$$c_{eff} = (u_{1_{sN}}c_{1N} + u_{2_{sN}}c_{2N})/u_0 \quad (53a)$$

(b) Two-phase case with downward gas flow in the dense phase

$$c_{eff} = c_{1_N} = c_{2_N} \quad (53b)$$

(c) Three-phase case with upward gas flow

$$c_{eff} = (u_{1_{sN}}c_{1N} + u_{2_{sN}}c_{2N} + u_{3_{sN}}c_{3N})/u_0 \quad (53c)$$

(d) Three-phase case with downward gas flow in the emulsion phase

$$c_{eff} = c_{3_N} = \frac{u_{1_{sN}}c_{1N} + u_{2_{sN}}c_{2N}}{u_{1_{sN}} + u_{2_{sN}}} \quad (53d)$$

Inlet Conditions

The equations devised before do not apply to the first compartment; the inlet condition is shown in Figures 4a and 4b.

(*a*) *Two-Phase Case.* If the two-phase model applies, $u_{1_{s0}}$ and $u_{2_{s0}}$ are calculated from Eqs. 11 and 12, i.e.,

$$u_{1_{s0}} = u_{1_{s1}} = \left(\frac{\epsilon_1 - \epsilon_{mf}}{1 - \epsilon_1}\right)0.711(gD_{1_1})^{1/2} \quad (54a)$$

$$u_{2_{s0}} = u_{2_{s1}} = u_0 - u_{1_{s0}} \quad (54b)$$

The aerosol mass balance equations are

Bubble Phase

$$Su_{1_{s0}}c_{in} + F_{v_1}c_{2_1} = Su_{1_{s1}}C_{1_1} + F_{v_1}c_{1_1} \quad (55a)$$

Dense Phase

$$Su_{2_{s0}}c_{in} + F_{v_1}c_{1_1} = Su_{2_{s1}}c_{2_1} + F_{v_1}c_{2_1} + u_{2_{s1}}c_{2_1}\left(\frac{1}{l}\right)\eta SD_{1_1} \quad (55b)$$

(*b*) *Three-Phase Case.* If three-phase model applies, $u_{1_{s0}}$, $u_{2_{s0}}$, and $u_{3_{s0}}$ are found from Eqs. 11, 22, and 23, i.e.,

$$u_{1_{s0}} = u_{1_{s1}} = \frac{\epsilon_1 - \epsilon_{mf}}{1 - \epsilon_1}0.711(gD_{2_1})^{1/2} \quad (56a)$$

$$u_{2_{s0}} = u_{2_{s1}} = u_{1_{s1}}\frac{\epsilon_{mf}\delta_{2_1}}{\delta_{1_1}} \quad (56b)$$

$$u_{3_{s0}} = u_{3_{s1}} = u_0 - u_{1_{s0}} - u_{2_{s0}} \quad (56c)$$

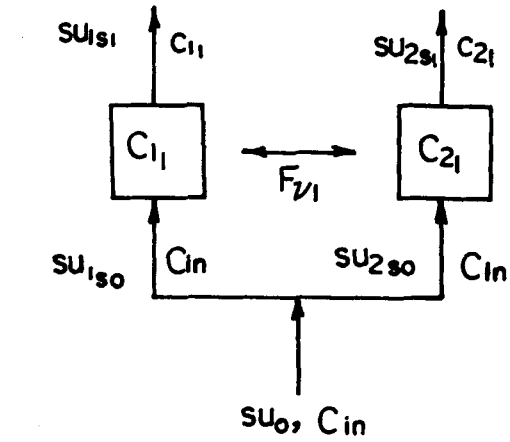

(a) Two - phase regime

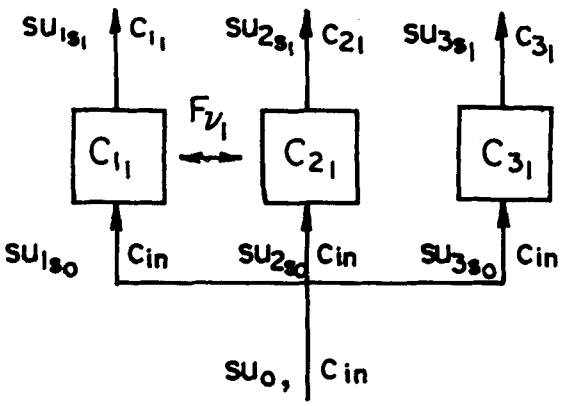

(b) Three-phase regime

Figure 4. Flow pattern of the first compartment.

The aerosol mass balance equations become
Bubble Phase

$$Su_{1_{s_0}}c_{\text{in}} + F_{v_1}c_{2_1} = Su_{1_{s_1}}c_{1_1} + F_{v_1}c_{1_1} \tag{57a}$$

Cloud Phase

$$Su_{2_{s_0}}c_{\text{in}} + F_{v_1}c_{1_1} = Su_{2_{s_1}}c_{2_1} + F_{v_1}c_{2_1} + u_{2_{s_1}}c_{2_1}\left(\frac{1}{l}\right)\eta S D_{2_1} \tag{57b}$$

Emulsion Phase

$$c_{3_1} = c_{\text{in}}e^{-\lambda D_{2_1}} \tag{57c}$$

METHOD OF CALCULATION

To estimate the performance of a particular fluidized filter, the sequence of calculations is as follows. First, the values of u_{mf}, ϵ_{mf}, and L are calculated (Appendix B) from the given conditions. The individual compartment height, D_{1_n} (or D_{2_n}), as a function of bed height; the volume fraction of the individual phases comprising the compartment; and gas velocities in the compartments can be calculated from the appropriate equations. In this step of calculation, care should be exercised in ascertaining the proper model to be used. The choice of the two-phase or the three-phase model is determined by the inequality condition of Eq. 9.

Once the series of bed compartments are specified, the values of aerosol concentration in each phase can be readily determined. The appropriate equations to be employed depend on both the number of phases involved and the direction of flow. As long as the flow of gas is upward, the calculation can be made incrementally, i.e., calculation of c_{i_n}'s based on the value of $c_{i_{n-1}}$'s. The number of equations involved at each step is not more than three. When the direction of the gas flow in the emulsion (or dense phase) is reversed, the aerosol concentration of a given phase in the nth compartment is now expressed by the aerosol concentrations in the preceding compartment, thus necessitating the simultaneous solutions of all these equations together with the equation describing the effluent concentrations (Eqs. 53a through 53d).

SAMPLE CALCULATIONS

The method presented in this work requires the use of a large number of model parameters. The way in which the model is structured, however, makes it difficult to obtain explicit relationships between these parameters and the performance of fluidized filters. Some understanding of the nature of the aerosol collection in fluidized filters can be discerned from the flow structure within the filter and the extent of aerosol collection on a compartment-to-compartment basis. The results of such a sample calculation are given below.

The results of the bed structure from sample calculations and the conditions under which they were made are summarized in Table 1. The extent of aerosol collection for each compartment can be seen from the compartment efficiency, E_n, defined as

$$E_n = \frac{c_{\text{eff}_{n-1}} - c_{\text{eff}_n}}{c_{\text{eff}_{n-1}}}$$

and

$$c_{\text{eff}_n} = \frac{\sum_i c_{\text{in}}u_{i_{sn}}}{u_0}$$

where the summation sign covers all the phases present in a compartment. The above definition requires modification in cases when reverse gas flow exists. The calculated results of E_n are given in Table 2.

The results given in Tables 1 and 2 indicate that the two-phase model applies to filters with relatively low bed height. The three-phase regime was observed in the case of L_{mf} = 16 cm and occurred in the top 1/3 of the bed. The bed structure changes moderately along the axial distance until it reaches L_{mf}. There is no change of δ_{1_n} for $h_n \leq L_{mf}$ as a consequence of Eq. 13a. The bubble-phase superficial gas velocity, on the other hand, increases by approximately 50%. This change in $u_{1_{sn}}$ has a substantial effect on filtration since there is no aerosol collection in the bubble phase. The most significant change occurs when $h_n > L_{mf}$, especially when there is a reversal of gas flow. It is questionable, though, whether reverse of flow of the magnitude predicted in the sample calculation for the last compartments (in cases of L_{mf} = 8 and 16 cm) does, indeed, occur. In terms of filter performance, this possible error is not important if the number of compartments is relatively large, Table 2.

The effect of gas interchange between the bubble and the cloud phases is believed to be of some significance since there is no aerosol collection in the bubble phase. (The effect of the gas interchange between the cloud and emulsion phases can be ignored because of its very small magnitude.) Available correlations of F_{12} differ significantly from one another. For example, the expression of Eq. 16, which was used by Peters et al. in modelling of catalytic fluidized reactors (Peters et al., 1982b), is only half as much as the equation used in their earlier work (Peters et al., 1982a).

As an indication of the effect due to the uncertainty in F_{12}, sample calculations using values of F_{12} from Eq. 16 as well as 2.25 times the value were made under otherwise identical conditions. The results of the total collection efficiency vs bed height are shown

TABLE 1. RESULTS OF SAMPLE CALCULATIONS ON FLUIDIZED-BED STRUCTURE

L_{mf} [10^{-2}m]	L [10^{-2}m]	n [—]	h_n [10^{-2}m]	D_{1_n} [10^{-2}m]	δ_{1_n} [—]	δ_{2_n} [—]	F_v [10^{-6}m^3/s]	$u_{1_{sn}}$ [10^{-2}m/s]	$u_{2_{sn}}$ [10^{-2}m/s]	Net Flow	Remarks
0.5	0.595	1	0.30	0.60	0.16	0.84	427.7	3.46	13.34	—	
1.0	1.18	1	0.34	0.68	0.155	0.845	471.3	3.37	13.43		
		2	0.93	0.50	0.155	0.845	300.2	3.63	13.17	1 ← 2	
2.0	2.35	1	0.34	0.68	0.148	0.852	449.0	3.18	13.62		
		2	1.09	0.82	0.148	0.852	449.0	3.49	13.31	1 ← 2	
		3	1.92	0.85	0.148	0.852	349.0	3.79	13.01	1 ← 2	
4.0	4.63	1	0.34	0.68	0.136	0.864	413.7	2.89	13.91		
		2	1.09	0.82	0.136	0.864	413.7	3.17	13.62	1 ← 2	
		3	1.99	0.98	0.136	0.864	413.7	3.47	13.33	1 ← 2	
		4	3.06	1.17	0.136	0.864	413.7	3.78	13.02	1 ← 2	
		5	4.14	0.99	0.304	0.696	676.7	11.28	5.52		
8.0	9.09	1	0.34	0.68	0.120	0.880	364.9	2.51	14.29		
		2	1.09	0.82	0.120	0.880	364.9	2.75	14.05	1 ← 2	
		3	1.99	0.98	0.120	0.880	364.9	3.00	13.80	1 ← 2	
		4	3.06	1.17	0.120	0.880	364.9	3.28	13.52	1 ← 2	
		5	4.33	1.38	0.120	0.880	364.9	3.57	13.23	1 ← 2	
		6	5.84	1.63	0.120	0.880	364.9	3.88	12.92	1 ← 2	
		7	7.61	1.91	0.120	0.880	364.9	4.20	12.60	1 ← 2	
		8	8.83	0.53	0.588	0.412	450.6	45.90	−29.10	1 ← 2	reverse flow in phase 2

L_{mf} [10^{-2}m]	L [10^{-2}m]	n [—]	h_n [10^{-2}m]	D_{1_n} [10^{-2}m]	D_{2_n} [10^{-2}m]	δ_{1_n} [—]	δ_{2_n} [—]	δ_{3_n} [—]	F_{v_n} [10^{-6}m^3/s]	$u_{1_{sn}}$ [10^{-2}m/s]	$u_{2_{sn}}$ [10^{-2}m/s]	$u_{3_{sn}}$ 10^{-2}m/s	Net Flow
16.0	17.8	1	0.34	0.68		0.101	0.899		308.1	2.07	14.73		
		2	1.09	0.82		0.101	0.899		308.1	2.27	14.53		1 ← 2
		3	1.99	0.98		0.101	0.899		308.1	2.48	14.32		1 ← 2
		4	3.06	1.17		0.101	0.899		308.1	2.71	14.09		1 ← 2
		5	4.33	1.38		0.101	0.899		308.1	2.95	13.85		1 ← 2
		6	5.84	1.63		0.101	0.899		308.1	3.20	13.60		1 ← 2
		7	7.61	1.91		0.101	0.899		308.1	3.47	13.33		1 ← 2
		8	10.69	2.37	4.26	0.101	0.488	0.410	554.1	3.86	7.07	5.68	1 ← 2 → 3
		9	15.16	2.98	4.66	0.101	0.286	0.612	481.8	4.33	4.65	7.82	1 ← 2 → 3
		10	17.65	3.29	0.32	0.639	0.251	0.110	187.1	71.51	10.68	−65.39	1 ← 2 ← 3

u_o = 0.168 m/s, u_{mf} = 0.12 m/s, D_R = 0.127 m, ϵ_{mf} = 0.38, N_D/s = 1.14 × 10^{-4} Nos. of Openings/m^2.

TABLE 2. CALCULATED RESULTS OF E_n

L_{mf} [10^{-2}m]	n	c_{1_n}	c_{2_n}	c_{3_n}	c_{eff_n}	E_n
0.5	1	0.911	0.819	—	0.838	0.162
1	1	0.894	0.799	—	0.818	0.182
	2	0.805	0.680	—	0.707	0.136
2	1	0.893	0.797	—	0.815	0.185
	2	0.752	0.621	—	0.648	0.205
	3	0.626	0.486	—	0.518	0.202
4	1	0.891	0.794	—	0.811	0.189
	2	0.747	0.616	—	0.641	0.210
	3	0.604	0.463	—	0.492	0.232
	4	0.474	0.338	—	0.369	0.250
	5	0.357	0.301	—	0.339	0.081
8	1	0.888	0.791	—	0.805	0.195
	2	0.741	0.609	—	0.631	0.216
	3	0.595	0.454	—	0.479	0.241
	4	0.463	0.326	—	0.353	0.263
	5	0.351	0.226	—	0.253	0.283
	6	0.260	0.152	—	0.177	0.300
	7	0.189	0.098	—	0.121	0.316
	8	0.066	0.038	—	0.066	0.455
16	1	0.885	0.787	—	0.799	0.201
	2	0.734	0.601	—	0.619	0.225
	3	0.585	0.443	—	0.464	0.250
	4	0.451	0.314	—	0.336	0.276
	5	0.338	0.214	—	0.236	0.298
	6	0.247	0.140	—	0.160	0.322
	7	0.177	0.088	—	0.106	0.338
	8	0.103	0.046	0.016	0.049	0.538
	9	0.064	0.026	0.004	0.026	0.469
	10	0.006	0.002	0.005	0.005	0.808

d_p = 1.6 × 10^{-6}m, D_c = 4.25 × 10^{-4}m, ρ_p = 1.05 × 10^{-3} kg/m^3, c_{in} = 1.

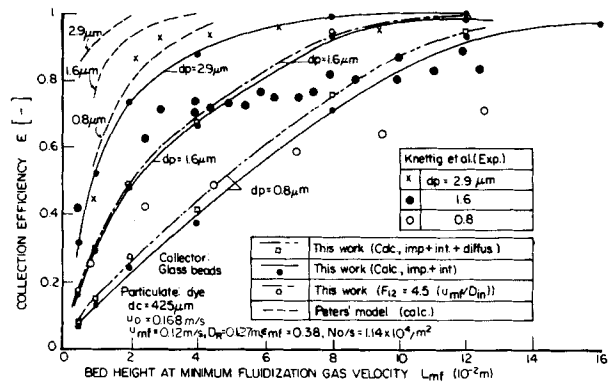

Figure 5a. Comparisons between calculated values and experimental data (Knettig et al., 1974) for overall collection efficiency as a function of bed height.

in Figure 5a. The difference in the collection efficiencies is very slight. This conclusion is consistent with the fact that the difference in particle concentration between bubble phase and dense phase is small, Table 2.

COMPARISON WITH PREVIOUS EXPERIMENTAL DATA

A number of investigators have reported the data on the performance of fluidized filters which can be used to assess the validity of the present method. In carrying out the comparisons, however, there are certain problems. First, the various experimental works do not necessarily have the same degree of accuracy; thus making it difficult to properly assess the meaning of agreement between

TABLE 3. EXPERIMENTAL DATA AGAINST WHICH PRESENT METHOD IS TESTED

Authors	Fig.	Collector	Particulate	u_o [10^{-2}m/s]	u_{mf} [10^{-2}m/s]	D_R [10^{-2}m]	L_{mf} [10^{-2}m]	ϵ_{mf} [—]	N_D/S [10^4No./m^2]	D_c [10^{-6}m]	d_p [10^{-6}m]	Remarks
Knettig et al. (1974)	5a	Glass beads	Monodispersed	16.8	12	12.7	0.5 ~ 125	0.38	1.14	425	0.8	
	a	Glass beads	dye particle	16.8	12	12.7	0.5 ~ 125	0.38	1.14	425	1.6	
	a	Glass beads	Monodispersed dye particle	16.8	12	12.7	0.5 ~ 125	0.38	1.14	425	2.9	
Doganoglue et al. (1978)	b	Glass beads	DOP	13	2	15	0.5 ~ 7	0.5	1.33	108	1.15	$u_{mf} >$ 0.2 m/s
McCarthy (1976)	c	Activated alumina	DOP	<4	1.56	5	5.1	0.5	89.5	175	0.67	Attribution of collector particles
				<4	1.56	5	5.1	0.5	89.5	175	1.4	
				<4	1.56	5	5.1	0.5	89.5	175	0.67	
Yankel (1972)	c	Activated alumina	DOP	<4	1.56	5	5.1	0.5	89.5	175	1.4	
Scott et al. (1959)	d	Silica gel	DOP	3 ~ 14	2(?)	5.1	6.3(?)	0.5	Screen	100(?)	0.87	Incomplete Information
		Silica gel	DOP	3 ~ 14	2(?)	5.1	12(?)	0.5	Screen	100(?)	0.87	
Meissner et al. (1949)	e	Silica gel	Sulfurica acid	30 ~ 90	0.357	4.7	17.4	0.5	0.058	67	5.3	Slug flow
		Activated alumina		30 > 1	0.756	4.7	22.7	0.5	0.058	120		

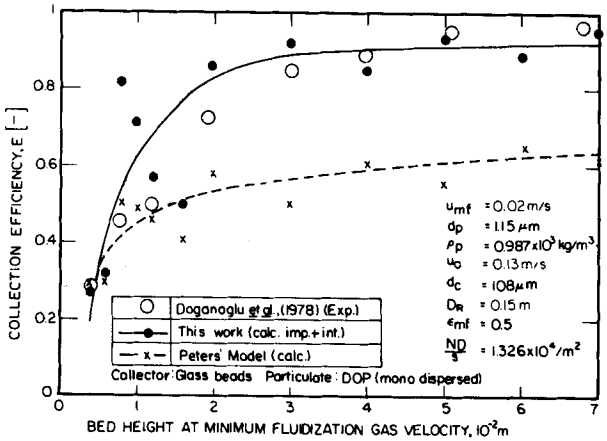

Figure 5b. Comparison between calculated values and experimental data (Doganoglu et al., 1978) for overall collection efficiency as a function of bed height.

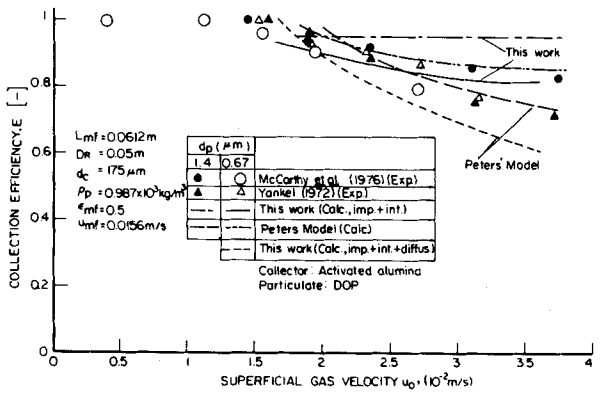

Figure 5c. Comparison between calculated values and experimental data (McCarthy et al., 1976; Yankel, 1972), for overall collection efficiency as a function of superficial gas velocity.

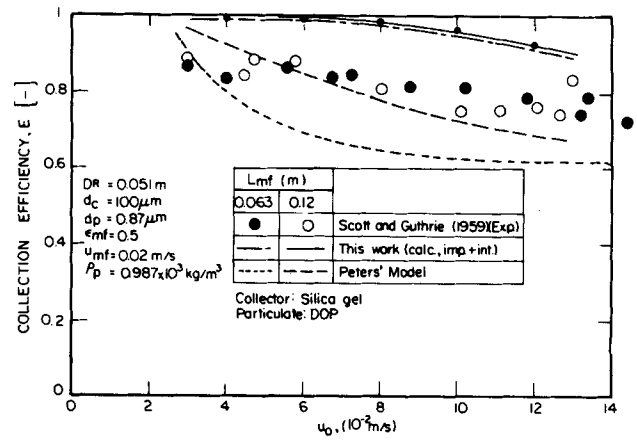

Figure 5d. Comparison between calculated values and experimental data (Scott and Guthrie, 1959) for overall collection efficiencies as a function of the superficial gas velocity.

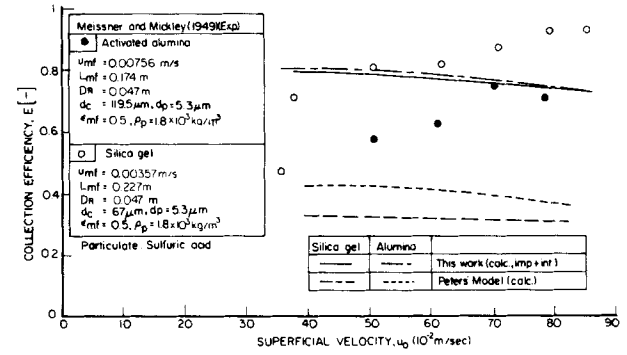

Figure 5e. Comparison between calculated values and experimental data (Meissner and Mickley, 1949) for overall collection efficiencies as a function of superficial gas velocity.

predictions from the present method and experimental data. Second, not all the information required in applying the present method was reported. Consequently, it was necessary to estimate, thereby introducing uncertainties. Finally, the present method is formulated on the basis that there is no significant particle reentrainment. Not all the experimental data used for comparison conforms to this requirement.

The experimental data against which the present method is tested consist of results from six separate investigators, Table 3. Comparisons between predictions based on the present method and experiments are shown in Figures 5a through 5e, as well as the predictions made using the three-phase model by Peters et al. (1982a). Discussions on the relative merit of these two methods are given in the following section.

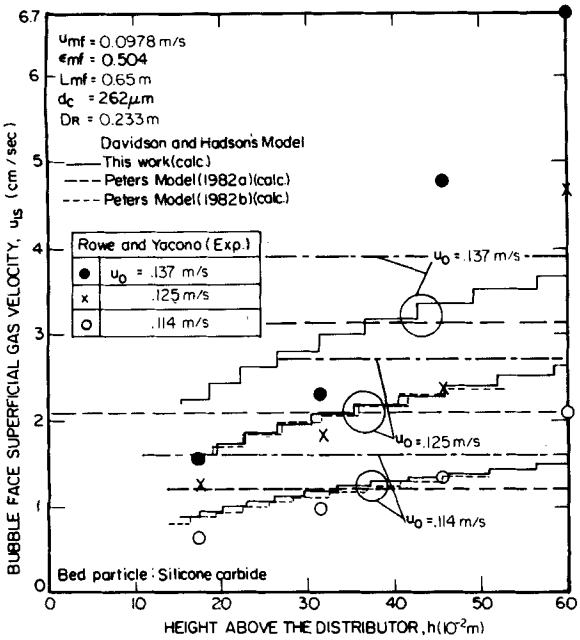

Figure 6a. Superficial bubble-phase gas velocity as a function of height from distributor.

The comparisons demonstrate that the present method yields essentially correct predictions. Generally, the predictions give somewhat higher values of the collection. The difference between prediction and experiment is within the range of accuracy of the data. Even though the degree of agreement observed does not necessarily constitute a validation of the method, it does provide some credence to the utility of the method for predicting fluidized filter performance.

Another comparison between the present method and experiment in the magnitude of bubble-phase superficial gas velocity is shown in Figure 6 which also includes the prediction made by Peters et al. (1982a,b). The experimental data are those reported by Rowe and Yacono (1976). The present method, similar to the method of Peters et al. (1982b), gives reasonably good agreement.

COMPARISON WITH METHOD OF PETERS ET AL.

As stated previously, the present method represents a natural extension of the work of Peters et al. (1982a). With the exception of one case (Figure 5d), it gives similar to much better agreement with experimental data than the method of Peters et al. The improvement of the present method over that of Peters et al., Figures 5a through 5e, on the other hand, is probably not significant in view of the uncertainties associated with model parameters and the limited accuracy of some of the experimental data.

There are, however, significant differences between the present method and that of Peters et al. These are mainly in three areas. The method of Peters et al. assumes that the three-phase model applies throughout the entire bed, and model parameters such as $u_{i_{sn}}$ and δ_{i_n} are constant. Calculations according to the procedures outlined by Peters et al., as pointed out earlier, may lead to the physically impossible situation where negative values of δ_{3_n} were obtained. (This happened when the three-phase model was applied to conditions shown in Figure 4d.) Eliminating the constant superficial velocity assumption as was done in this work provides a more general description and allows for the net flow of gas from one phase to another, which may take place in two ways, interchange and net flow. Based on these considerations, one may argue that the present method, compared to that of Peter et al., provides a more realistic bed structure. Another difference between the present method and the earlier work is the description of the flow

TABLE 4. COMPARISONS BASED ON TWO DIFFERENT COLLECTOR GEOMETRIES

$d_p = 0.1\ \mu m$	Present Method*		Peters Model†
	Mixing	No Mixing	
E	0.1146	0.1216	0.1183
	$\eta_{imp+int} = 6.05 \times 10^{-4}$		$\eta_{imp} = 9.6 \times 10^{-8}$
	$\eta_{BD} = 4.6 \times 10^{-3}$		$\eta_{int} = 7.1 \times 10^{-4}$
	$\eta = 5.2 \times 10^{-3}$		$\eta_{BD} = 1.03 \times 10^{-3}$
			$\eta_E = 5.64 \times 10^{-5}$
			$\eta = 6.1 \times 10^{-3}$
$d_p = 0.5\ \mu m$	Present Method*		Peters Model†
	Mixing	No Mixing	
E	0.0959	0.1009	0.2783
	$\eta_{imp+int} = 3.68 \times 10^{-3}$		$\eta_{imp} = 1.35 \times 10^{-5}$
	$\eta_{BD} = 5.86 \times 10^{-4}$		$\eta_{int} = 3.53 \times 10^{-3}$
	$\eta = 4.27 \times 10^{-3}$		$\eta_{BD} = 2.08 \times 10^{-4}$
			$\eta_E = 1.4 \times 10^{-3}$
			$\eta = 0.0176$
$d_p = 1.5\ \mu m$	Present Method*		Peters Model†
	Mixing	No Mixing	
E	0.280	0.323	0.6446
	$\eta_{imp+int} = 1.558 \times 10^{-2}$		$\eta_{imp} = 8.37 \times 10^{-4}$
	$\eta_{BD} = 3.97 \times 10^{-4}$		$\eta_{int} = 1.06 \times 10^{-2}$
	$\eta = 1.597 \times 10^{-2}$		$\eta_{BD} = 8.87 \times 10^{-5}$
			$\eta_E = 1.27 \times 10^{-2}$
			$\eta = 8.29 \times 10^{-2}$
$d_p = 5\ \mu m$	Present Method*		Peters Model†
	Mixing	No Mixing	
E	0.700	0.914	0.9446
	$\eta_{imp+int} + 9.38 \times 10^{-2}$		$\eta_{imp} = 4.86 \times 10^{-2}$
	$\eta_{BD} = 1.68 \times 10^{-4}$		$\eta_{int} = 3.53 \times 10^{-3}$
	$\eta = 9.4 \times 10^{-2}$		$\eta_{BD} = 3.76 \times 10^{-5}$
			$\eta_E = 1.41 \times 10^{-1}$
			$\eta = 0.77$

* The collection efficiencies due to various mechanisms were calculated according to the expressions given in Appendix C.

† The collection efficiencies were calculated according to the expressions used by Peters et al. (1982a).

$u_o = 0.15$ m/s, Bed Height = 0.01m, $\epsilon_{mf} = 0.38$, $d_c = 425\ \mu m$, $\rho_p = 0.987 \times 10^3$ kg/m^3, $\epsilon_D = 8.5$, $Q_{AC} = 2.65 \times 10^{-7}$ c/m^2.

condition in the emulsion phase. Peter et al. considered that the aerosol concentration is uniform in both the emulsion and the cloud phases. In contrast, in the present work uniform aerosol concentration is supposedly maintained only in the cloud phase. The emulsion phase is considered to be similar to a packed bed with a porosity of ϵ_{mf} and negligible axial dispersion. This assumption is believed to be more realistic in view of the recent study on magnetically stabilized fluidized filtration (Albert, 1982).

The extent of aerosol collection in the present work is estimated by approximating the dense phase (emulsion or cloud) with the use of the constricted tube model and the Pendse-Tien correlation for η(or λ). The major mechanisms of aerosol collection were inertial impaction, interception, and Brownian diffusion for submicron particles. In contrast, Peters et al. used the isolated sphere model for estimating aerosol collection in the dense phase. The dominant mechanisms were assumed to be the same as those considered in the present work plus collection resulting from induced electrostatic force. The use of the isolated sphere model to describe aerosol collection in granular media, however, is known to be inadequate (Tien, 1982; Pendse and Tien, 1982).

The use of different collector geometries in these two methods also leads to significant differences in estimating the collection efficiencies of the unit cell (or single collector). This point can be seen from the sample calculations shown in Table 4. The calculations were made by considering the collection efficiency of a single compartment of height of 1 cm composed of the dense phase only with $d_c = 425\ \mu m$, $d_p = 0.1$, 0.5, 1.5 and 5 μm, $u_0 = 15$ cm/s, and $\epsilon_{mf} = 0.38$. Included in Table 4 are the values of the unit cell (or single collector) efficiencies due to different collection mechanisms

as well as the total collection efficiency of the compartment E. If the dense phase is considered to be a packed bed, with plug flow and with no axial dispersion, E is given as

$$E = 1 - \frac{c_{\text{eff}}}{c_{\text{in}}} = 1 - e^{-\eta/lL} \tag{58}$$

On the other hand, if the aerosol concentration is assumed to be uniform, E becomes

$$E = [1 + l/L\eta)]^{-1} \tag{59a}$$

with the use of the constricted tube model, and

$$E = \left[1 + \frac{2D_c}{3\eta(1 - \epsilon_{mf})L}\right]^{-1} \tag{59b}$$

with the use of the spherical collector model.

It is clear from the above expressions that for the same value of η, a greater E is predicted if the well-mixed assumption is not employed.

The expressions used by Peters et al. in calculating the collection efficiency that results from inertial impaction and interception are

$$\eta_{\text{Imp}} = \frac{N_{st}^2}{(N_{st} + 1/2)^2} \tag{60}$$

$$\eta_{\text{int}} = (1 + N_R)^2 - \frac{1}{1 + N_R} \tag{61}$$

Equation 60 is known to give gross underestimation, as shown by the work of Tien (1982) and Pendse and Tein (1982). On the other hand, η_{Int} according to Eq. 61 is proportional to N_R for small values of N_R. This expression was obtained on the basis of the potential flow. Similar expressions based on viscous flow show that $\eta \sim N_R$. In granular filtration, N_R is usually of the order 10^{-2} to 10^{-1}; the use of Eq. 61 leads to overestimation by at least one order of magnitude. A compensating effect is achieved in this case. However, there is no assurance that it will exist in all cases.

Two other points concerning the calculation of η in the work of Peters et al. deserve further comment. First, the use of the correction factor, $g(\epsilon) = 1.3/\epsilon_{mf}$, to extend the results of the isolated sphere model to the dense phase is valid only for Brownian particles. Its use in cases where inertial impaction and/or interception are important is questionable. Second, the calculation of the collection efficiency due to induced electrostatic effect, η_E, can be made only very approximately. η_E is shown to be proportional to the 0.8 power of the charge density of the dielectric bed medium. The value of the charge density of the medium is generally unavailable and, therefore, has to be estimated. Peters et al. chose the value to be two orders of magnitude less than the maximum value for surfaces charged in air. A difference by a factor of two, however, would cause an uncertainty of approximately 60% in the calculated value of η_E, which in turn would change the value of E, Table 4, more than 20%.

ACKNOWLEDGMENT

This study was performed under Contract No. DE-AC02-79-ER16386, Department of Energy.

APPENDIX A

The bubble velocity u_1 may be assumed to be the sum of the bubble rising velocity, which is given to be $0.711\sqrt{gD_1}$ and the upward velocity of the dense phase between bubbles. If there is no bubbles, or $u_{1_s} = 0$ cm/s, the dense phase, on the average, does not have any upward velocity. On the other hand, if bubbles are continuously generated at the bottom of the bed, the dense phase between bubbles must have a mean upward velocity equal to u_{1_s}. Accordingly

$$u_{1_n} = u_{1_{sn}} + 0.711\sqrt{gD_{1_n}} \tag{A1}$$

In contrast, Davidson and Harrison (1963) argued that u_{1_n} can be expressed as

$$u_{1_n} = (u_o - u_{mf}) + 0.711\sqrt{gD_{1_n}} \tag{A2}$$

Both equations give essentially the same results if u_o and u_{mf} are of the same order of magnitude and δ_{1_n} remains a relatively small quantity. Both of these conditions are met in fluidized filtration.

APPENDIX B: CORRELATIONS USED TO ESTIMATE ϵ_{mf} AND u_{mf}

According to Wen and Yu (1966) the minimum fluidization velocity, u_{mf} and the bed porosity at u_{mf} can be estimated from the following expressions

$$u_{mf} = \frac{(d_c^2)(\rho_s - \rho)g}{1{,}650\mu} \quad N_{Re_p} < 20 \tag{B1}$$

$$u_{mf}^2 = \frac{(d_c)(\rho_s - \rho)g}{24.5\rho} \quad N_{Re_p} > 1{,}000 \tag{B2}$$

$$\frac{1 - \epsilon_{mf}}{\phi_s^2 \epsilon_{mf}^3} \simeq 11 \quad N_{Re_p} < 20 \tag{B3}$$

$$\frac{1}{\phi_s \epsilon_{mf}^2} \simeq 14 \quad N_{Re_p} > 1{,}000 \tag{B4}$$

where ϕ_s is the shape factor defined as the ratio of the surface area of a sphere which has the same volume of the fluidized particles to that of the particle.

APPENDIX C: COLLECTION EFFICIENCIES OF UNIT CELLS OF GRANULAR MEDIA

In a recent study, Pendse and Tien (1982) presented a general correlation for the estimation of the collection efficiency due to inertial impaction and interception of unit cells constituting a granular medium. Their result is given as

$$\eta_{I,i} = (1 + 0.004 + N_{Re_s})\left[N_{st} + 0.48\left(4 - \frac{N_R}{d_c^*} - \frac{N_R^2}{d^{*2}}\right)^{1/2}\left(\frac{N_R^{1.0412}}{d_c^*}\right)\right] \tag{C1}$$

$$N_{Re_s} = d_c u_o \rho/\mu \tag{C2}$$

$$N_{st} = d_p^2(\rho_p - \rho)gc_s/9\mu u_0 \tag{C3}$$

$$N_R = d_p/d_c \tag{C4}$$

and d_c^* is the dimensionless constriction diameter and can be determined from the saturation-capillary pressure data. As an approximation, d_c^* may be taken to be 0.35.

The unit cell collection efficiency due to Brownian diffusion, η_{BD} has been evaluated by Chiang and Tien (1982). For $0.37 < \epsilon < 0.47$ η_{BD} is found to be

$$\eta_{BM} = 7.3808\epsilon^{-0.5864}(1 - \epsilon)^{2/3} N_{Pe}^{-1/3} \tag{C5}$$

where

$$N_{Pe} = d_c u_o / D_{BM} \tag{C6}$$

NOTATION

c_{eff} = particle concentration of aerosol leaving a filter bed or a compartment, particulate volume/aerosol volume
c_{in} = particle concentration of aerosol entering a filter bed or a compartment
c_{i_n} = particle concentration of aerosol in the ith phase of nth compartment
C_s = Cunningham's slip factor
d_c = diameter of filter grain

d_p = particle diameter of aerosol, m
D_1 = equivalent spherical bubble diameter, having the same volume as that of a bubble, m
D_{1_n} = diameter of gas bubble in nth compartment, m
D_{1_0} = initial gas bubble diameter, m
D_{1_m} = maximum gas bubble diameter, m
D_{2_n} = equivalent spherical cloud diameter in nth compartment, m
D_B = Brownian diffusivity
D_R = fluid bed diameter, m
E = overall collection efficiency
E_n = collection efficiency of the nth compartment
F_{12_n} = gas interchange coefficient between phase 1 and phase 2 per unit volume of phase 1 in the nth compartment, L/s
F_{v_n} = $F_{12_n}V_{1_n}$, m^3/s
g = gravitational acceleration, m/s^2
$g(\epsilon)$ = correction factor
h = height from distributor plate, m
h_n = height of the center of nth compartment from distributor plate, m
l = length of unit bed element, m
L = expanded bed height, m
L_{mf} = bed height at minimum fluidization gas velocity, m
m_c = number of particles collected in a unit cell
m_{in} = number of particles entered in a unit cell
M_{2_n} = rate of particle collection in phase 2 of the nth compartment
N_c = number of constricted tubes per unit bed cross sectional area, L/m^2
N_D = number of orifices on the distributor
N_R = relative size parameter, d_p/d_c
N_{Re_s} = Reynolds number, $D_c u_o \rho/\mu$
N_{sh} = Sherwood number
N_{St} = Stokes' number, $d_p^2 u_o \rho_p c_s/9\mu d_c$
Q_{Ac} = charge density of the bed medium, C/cm^2
q = volumetric flow rate per unit cell, m^3/s
S = cross-sectional area of bed, m^2
u_o = superficial gas velocity, m/s
u_{1_n} = rising velocity of a bubble in nth compartment, m/s
$u_{i_{s_n}}$ = superficial gas velocity in phase i in nth compartment, m/s
u_{mf} = minimum fluidization velocity, m/s
V_{1_n} = volume of bubble phase in nth compartment, m^3

Greek Letters

δ_{i_n} = volume fraction of bed occupied by phase i
ϵ = bed porosity
ϵ_D = dielectric constant of aerosol particle
ϵ_n = porosity in nth compartment
ϵ_{i_n} = porosity in phase i in nth compartment
η = collection efficiency of unit bed element
η_{BM} = collection efficiency contribution due to Brownian diffusion
η_E = collection efficiency contribution due to induced electrostatic force
η_{imp} = collection efficiency contribution due to particle inertia
$\eta_{imp+int}$ = collection efficiency contribution due to particle inertia and interception
η_{int} = collection efficiency contribution due to interception
λ = filter coefficient, L/m
μ = viscosity of gas, $N/s\cdot m^2$
ρ = density of gas, kg/m^3
ρ_s = density of collector particle, kg/m^3
ρ_p = density of a particle of aerosol, kg/m^3
σ = specific deposit
ϕ_s = shape factor as calculating ϵ_{mf}

LITERATURE CITED

Albert, R., "Dust Filtration with a Magnetically Stabilized Fluidized Bed," M.S. ChE. Thesis, Syracuse Univ., Syracuse, NY (1982).
Chiang, H. W., and C. Tien, "Deposition of Brownian Particles in Packed Beds," *Chem. Eng. Sci.*, **37**, 1159 (1982).
Ciborows, J., and L. Zakowski, "Dust Removal in a Fluidized Bed. II. Electrostatic Effects in a Fluidized Bed and Their Effect on Dust-Removal Process Efficiency," *Int. Chem. Eng.*, **17**, 538 (1977).
Ciborovsky, J., and A. Wlodarsky, "On Electrostatic Effects in Fluidized Beds," *Chem. Eng. Sci.*, **17**, 23 (1962).
Davidson, J. F., and D. Harrison, *Fluidized Particles*, Cambridge Univ. Press (1963).
Doganoglu, Y., V. Jog, D. V. Thambimuthu, and R. Clift, "Removal of Fine Particulates from Gases in Fluidized Beds," *Trans. Inst. Chem. Eng.*, **56**, 239 (1978).
Juvinall, R. A. R., K. Kessie, and M. J. Steindler, "Sand-Bed Filtration of Aerosols", A Review of Published Information on Their Use in Industrial and Atomic Facilities," ANL-7683, Argonne National Laboratory (1970).
Kato, K., and C. Y. Wen, "Bubble Assemblage Model for Fluidized Bed Catalytic Reactors," *Chem. Eng. Sci.*, **24**, 1351 (1969).
Knettig, P., and J. M. Beeckmans, "Capture of Monodispersed Aerosol Particles in a Fixed and in a Fluidized Bed," *Can J. Chem. Eng.*, **52**, 703 (1974).
Kunii, D., and O. Levenspiel, "Bubbling Bed Model. Model for Flow of Gas through a Fluidized Bed," *Ind. Eng. Chem. Fund.*, **7**, 446 (1968).
McCarthy, D., A. J. Yankel, R. G. Patterson, and M. L. Jackson, "Multistage Fluidized Bed Collection of Aerosols," *Ind. Eng. Chem. Process Des. Dev.*, **15**, 266 (1976).
Meissner, H. P., and H. S. Mickley, "Removal of Mists and Dusts from Air by Beds of Fluidized Solids," *Ind. Eng. Chem.*, **41**, 1238 (1949).
Mori, S., and C. Y. Wen, "Estimation of Bubble Diameter in Gaseous Fluidized Beds," *AIChE J.*, **21**, 109 (1975).
Murray, J. D., "On the Mathematics of Fluidization. Part 2. Study Motion of Fully Developed Bubbles," *Fluid Mech.*, **22**, 57 (1965).
Patterson, R. G., and M. L. Jackson, "Shallow Multistage Fluidized Beds for Particle Collection," *AIChE Symp. Ser.*, No. 161, **73**, 64 (1977).
Payatakes, A. C., C. Tien, and R. M. Turian, "A New Model for Granular Porous Media—Part 1. Model Formulation," *AIChE J.*, **19**, 58 (1973).
Peters, M. H., L.-S. Fan, and T. L. Sweeney, "Simulation of Particulate Removal in Gas-Solid Fluidized Beds," *AIChE J.*, **28**, 39 (1982a).
Peters, M. H., L.-S. Fan, and T. L. Sweeney, "Reactant Dynamics in Catalytic Fluidized Bed Reactors with Flow Reversal of Gas in the Emulsion Phase," *Chem. Eng. Sci.*, **37**, 553 (1982b).
Pilney, J. P., and E. E. Erikson, "Final Report on Removal of Flyash by Fluidized Bed Techniques," Contract No. 14-69-0070-375 to U.S. Department of Interior Bureau of Mines (March 8, 1968a).
Pilney, J. P., and E. E. Erikson, "Fluidized Bed Flyash Filter," *J. Air Pollut. Cont. Assoc.*, **18**, 684 (1968b).
Rowe, P. N., and C. R. X. Yacono, "The Bubbling Behavior of Fine Powders When Fluidized," *Chem. Eng. Sci.*, **31**, 1179 (1976).
Scott, D. S., and D. A. Gurthrie, "Removal of a Mist in a Fluidized Bed," *Can. J. Chem. Eng.*, 20 (Oct., 1959).
Sit, S. P., and J. R. Grace, "Effect of Bubble Interaction and Interphase Mass Transfer in Gas Fluidized Beds," *Chem. Eng. Sci.*, **36**, 327 (1981).
Tien, C., "Aerosol Filtration in Granular Media," *Chem. Eng. Commu.*, **17**, 361 (1982).
Tien, C., and A. C. Payatakes, "Advances in Deep Bed Filtration," *AIChE J.*, **25**, 737 (1979).
Wen, C. Y., and Y. H. Yu, "Mechanics of Fluidization," *Chem. Eng. Prog. Symp. Ser.*, **62**, 100 (1966).
Yankel, A. J., "Fine Particle Collection with a Fixed-Fluidized Bed," M.S. ChE. Thesis, University of Idaho, Moscow, ID (1972).
Zahedi, K., and J. R. Melcher, "Electrofluidized Beds in the Filtration of a Submicron Aerosol," *J. Air Pollut. Cont. Ass.*, **26**, 345 (1976).
Zahedi, K., and J. R. Melcher, "Collection of Submicron Particles in Bubbling Electro-Fluidized Beds," *Ind. Eng. Chem. Fund.*, **16**, 248 (1977).

Manuscript received November 8, 1982; revision received April 4, and accepted April 15, 1983.